Notes

SU-8-based Flexible Amperometric Device with IDA Electrodes to Regenerate Redox Species in Small Spaces

Yusuke KANNO,* Takehito GOTO,* Kosuke INO,*† Kumi Y. INOUE,* Yasufumi TAKAHASHI, Hitoshi SHIKU,* and Tomokazu MATSUE*,**†**

**Graduate School of Environmental Studies, Tohoku University, 6-6-11 Aramaki, Aoba, Sendai 980–8579, Japan*
***WPI-Advanced Institute for Materials Research, Tohoku University, 6-6-11 Aramaki, Aoba, Sendai 980–8579, Japan*

A flexible sensor based on SU-8 photoresist was fabricated and its electrochemical performance was investigated using cyclic voltammetry. The device consisted of interdigitated array (IDA) electrodes on an SU-8 layer. It exhibited a clear electrochemical response during redox cycling of ferrocenemethanol at the IDA electrodes. Since the device was flexible, it could be inserted into a narrow bent space to monitor electrochemical responses. The observed electrochemical behavior was found to be consistent with that predicted by simulations based on redox compound diffusion.

Keywords Electrochemical detection, amperometric sensor, flexible device, interdigitated array (IDA) electrodes, redox cycling

(Received September 14, 2013; Accepted November 20, 2013; Published February 10, 2014)

Introduction

Several kinds of flexible sensors have been developed for bioapplications,[1-6] with parylene or poly(dimethylsiloxane) (PDMS) most commonly being used as the flexible substrate. For highly sensitive comprehensive assays, a CMOS-based sensor and an electrode array device have been fabricated on flexible substrates.[7] Because of their flexibility and biocompatibility, such devices have been used to stimulate nerves and detect synaptic activity, and also as amperometric sensors for purposes such as glucose detection in the human body.

During *in vivo* amperometric detection, the analytes often need to be measured in narrow spaces. However, conventional amperometric sensors are not suitable for such measurements because in narrow confined spaces, the redox compound is rapidly consumed during electrochemical detection. Therefore, processes involving signal amplification and regeneration of the redox compound are preferable for reliable measurements. One method of signal amplification is redox cycling on interdigitated array (IDA) electrodes. Such electrodes have two interdigitated comb-type arrays consisting of planar parallel fingers.[8–16] When a suitable potential is applied to each electrode, species that become oxidized at one electrode finger are regenerated at neighboring fingers, resulting in redox cycling for amplification of the electrochemical signal. Such IDA electrodes have been applied for electrochemical detection of enzyme activity,[8–13] and have also been fabricated on a gas-permeable membrane to produce a gas-sensing system.[17]

† To whom correspondence should be addressed.
E-mail: ino.kosuke@bioinfo.che.tohoku.ac.jp (K. I.); matsue@bioinfo.che.tohoku.ac.jp (T. M.)

In the present study, IDA electrodes were incorporated into a flexible device for electrochemical detection in narrow spaces. An epoxy-based negative photoresist (SU-8) was chosen for the flexible substrate because it is a common material with well-known properties. As a demonstration toward bioanalysis in small spaces, the device was bent and inserted into a groove in an acrylic resin block, and ferrocenemethanol ($FcCH_2OH$) in the groove was then detected using redox cycling. The results were compared with those obtained from simulations, in order to evaluate the utility of such a sensor in small spaces.

Experimental

Device fabrication

A schematic of the device fabrication process is shown in Fig. 1. First, SU-8 3025 (MicroChem Co., USA) was spin-coated at 3000 rpm for 30 s onto a glass slide (Matsunami Glass Ind. Ltd., Japan). The substrate was then heated in two steps on a hotplate (65°C, 1 min; 95°C, 15 min). After cooling, the substrate was irradiated with UV light for 28 s through a patterned chromium mask. After exposure, the substrate was again heated in two steps on the hotplate (65°C, 1 min; 95°C, 5 min). Following cooling, the pattern was developed using an SU-8 developer (MicroChem) to appear the SU-8 layer (length, 28 mm; width, 16 mm; thickness, 25 μm), and the substrate was hard baked at 145°C for 20 min. Ti/Pt (thickness: 75 nm/110 nm) was then sputtered onto the SU-8 layer to fabricate IDA electrodes and a Pt counter electrode on the device. The additional electrodes were masked with ELEGRIP tape (thickness, 80 μm; DENKA, Japan) to form a rectangular window (10 mm × 5.0 mm) that exposed only the IDA electrodes. The SU-8-based device with the IDA electrodes was peeled from the glass slide with tweezers. The IDA electrodes

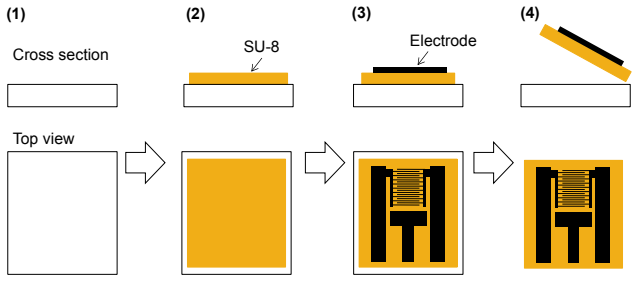

Fig. 1 Schematic illustration of device fabrication process. (1) Glass slide. (2) SU-8 layer. (3) IDA and counter electrodes. (4) The device could be peeled off from the glass slide. The additional electrodes were masked with tape in order to insulate them.

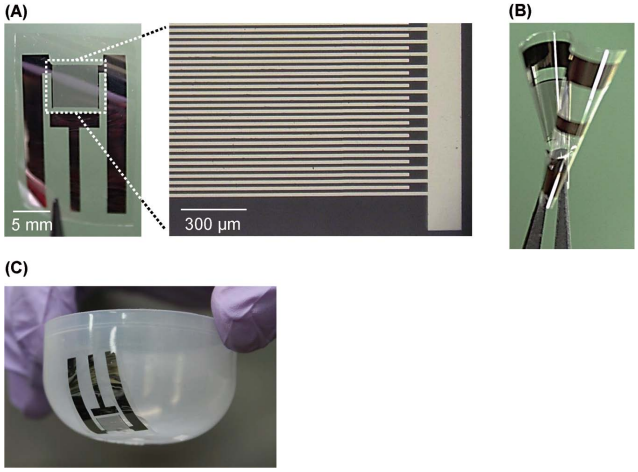

Fig. 2 (A) Photograph of the device and optical micrograph of the IDA electrodes. The thickness of the device was 25 µm. The width of the electrodes and the gap between them were 16 and 14 µm, respectively. (B) Device being bent with a tweezers. (C) Device attached to a curved surface.

had two interdigitated comb-type arrays consisting of 193 fingers with widths and lengths of 16 µm and 5.0 mm, respectively, and separations of approximately 14 µm.

Electrochemical measurements

Before the device was peeled from the glass slide, it was characterized by cyclic voltammetry in single and dual modes. The device was connected to a multichannel potentiostat (HA-1010 mM4, Hokuto Denko, Japan) and a 500-mM Tris–HCl buffer (pH 9.5) containing 1.0 mM $FcCH_2OH$ was then introduced onto the device. An Ag/AgCl reference electrode and a Pt wire counter electrode were inserted into the solution. Measurements were carried out using the external Pt counter electrode. In single mode, both electrodes were scanned from 0.00 to 0.50 V and the response was acquired from one electrode. In dual mode, one electrode (generator) was scanned from 0.00 to 0.50 V, while the other electrode (collector) was held at 0.00 V. After peeling the device from the glass slide, the device was then inserted into a 1.2-mm-wide bent groove in an acrylic resin block (AP-1000, Acrysunday Co., Ltd.). The bent groove in the acrylic resin block was fabricated using a CO_2 laser system (Universal Laser Systems Inc.). The groove was filled with the Tris–HCl buffer containing 1.0 mM $FcCH_2OH$, and cyclic voltammetry in single and dual modes was performed.

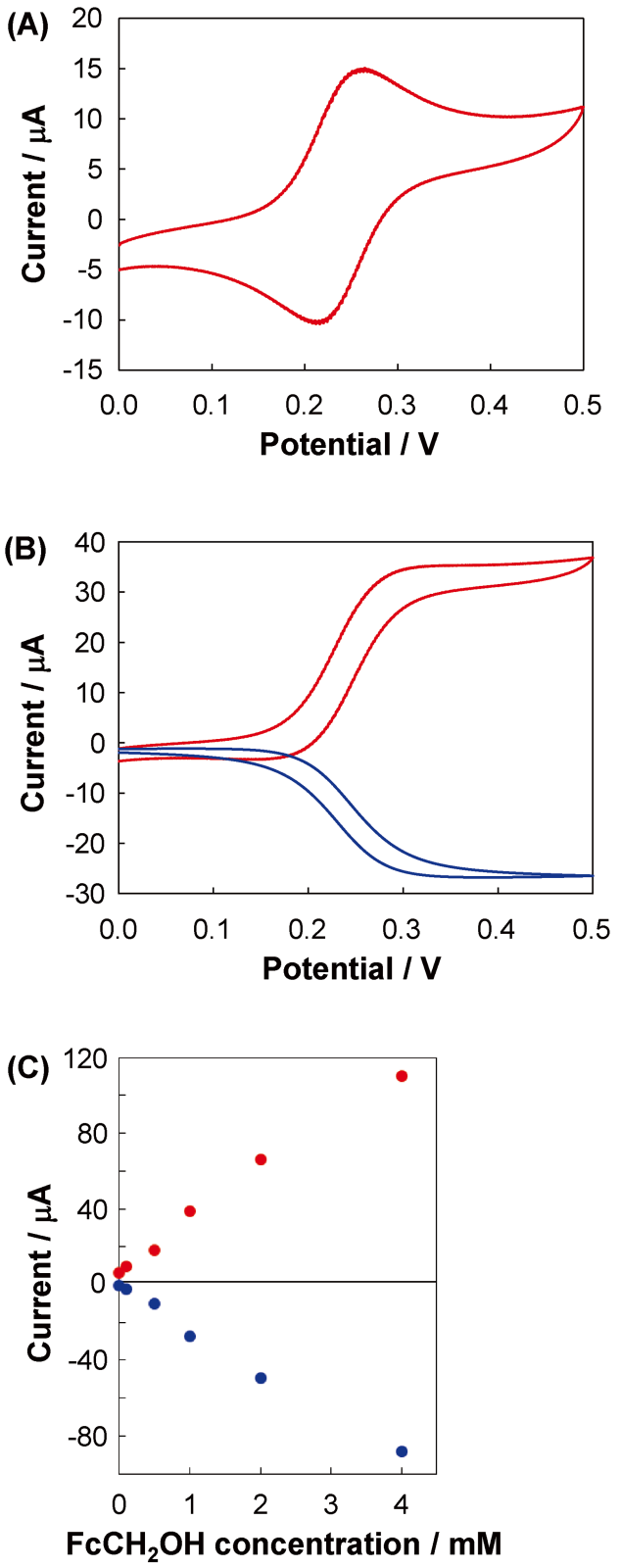

Fig. 3 Electrochemical detection using a device on a glass slide. Cyclic voltammograms for 1.0 mM $FcCH_2OH$ in single (A) and dual (B) modes. In single mode, both electrodes were scanned from 0.00 to 0.50 V at 20 mV/s and the response was acquired from one electrode. In dual mode, one electrode (generator, red) was scanned from 0.00 to 0.50 V at 20 mV/s, while the other electrode (collector, blue) was held at 0.00 V. (C) Dependence of the generator (red) and collector currents (blue) at 0.50 V on the $FcCH_2OH$ concentration (0, 0.10, 0.50, 1.0, 2.0, and 4.0 mM).

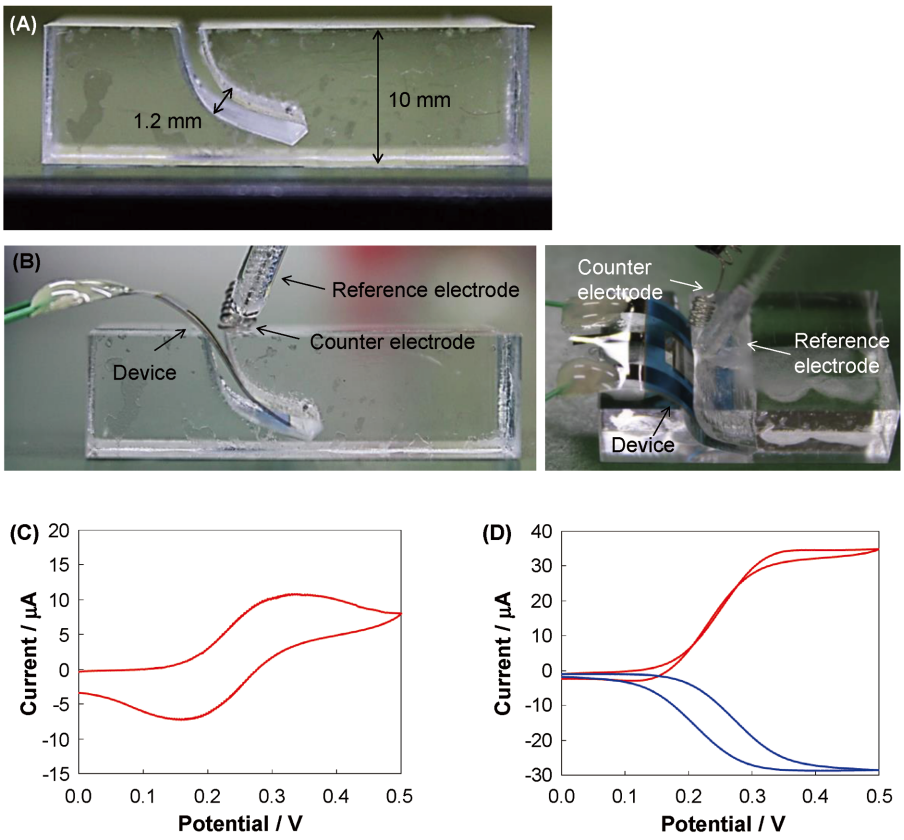

Fig. 4 Electrochemical detection using a flexible device peeled from a glass substrate in a narrow groove. (A) Photograph of acrylic resin block with groove. The depth and length of the groove were 9.1 and 11 mm, respectively. (B) Photograph of device inserted into the groove. Cyclic voltammograms for 1.0 mM $FcCH_2OH$ in single (C) and dual (D) modes. In single mode, both electrodes were scanned from 0.00 to 0.50 V at 20 mV/s and the response was acquired from one electrode. In dual mode, one electrode (generator, red) was scanned from 0.00 to 0.50 V at 20 mV/s, while the other electrode (collector, blue) was held at 0.00 V.

All electrochemical experiments were performed in a Faraday cage to reduce electromagnetic interference.

Simulation of current due to redox compound diffusion

The redox current at the IDA electrodes was calculated using COMSOL Multiphysics 4.3b (COMSOL, Inc., Sweden) using the method described in our previous paper.[9] Briefly, IDA electrodes were arranged at the bottom of 3D models with different channel heights, in order to investigate the effect of confined spaces. The electrochemical system was assumed to correspond to a reversible one-electron-transfer reaction. As an initial condition, the model was filled with 1.0 mM of the reduced analyte ($FcCH_2OH$). The diffusion coefficients of the oxidized ($FcCH_2OH^+$) and reduced forms ($FcCH_2OH$) of the analyte were set to the same value (7.0×10^{-10} m^2/s),[18] indicating that the sum of the concentrations of the oxidized and reduced forms was equal to the initial concentration of the analyte.[19,20] The concentrations of the oxidized and reduced forms at the electrode during the electrochemical reaction were calculated using the Nernst equation. The standard electrode potential of the redox compound was set to 0.216 V.

Results and Discussion

As shown in Fig. 2A, the device was successfully peeled from the glass slide. Since the device was very flexible, it can be bent without fracturing (Fig. 2B) and attached to a rounded surface (Fig. 2C). However, the SU-8 layer exhibits lower mechanical stability than a parylene layer, and adheres more strongly to glass than does parylene. In particular, it was found that reducing the time and temperature of the hard bake made it easier to peel the device from the glass. This was why baking was carried out for 20 min at 145°C, rather than 30 min at 180°C. Compared to a parylene-based device, it is easy to fabricate a thick SU-8-based device (>100 µm) by changing the spin speed for coating an SU-8 resist. In addition, several kinds of SU-8 patterns can be easily fabricated using only conventional lithography. The SU-8 3000 data sheet describes that the tensile strength and Yong's modules of SU-8 are approximately 73 MPa and 2.0 GPa, respectively, and the thermal stability (5% weight loss temperature) of SU-8 is approximately 300°C. Since SU-8 is used as an etch mask in both wet and dry processes, its chemical resistance is excellent.

Figures 3(A) and 3(B) show cyclic voltammograms for $FcCH_2OH$ in single and dual modes, respectively, using the SU-8-based device with the IDA electrodes before peeling it from the glass slide. It can be seen that the oxidation current of $FcCH_2OH$ is higher in dual mode than in single mode, indicating that the electrochemical signals were successfully amplified by redox cycling. For a current of 0.50 V, the collection efficiency and the signal amplification ratio were calculated to be 71.9%

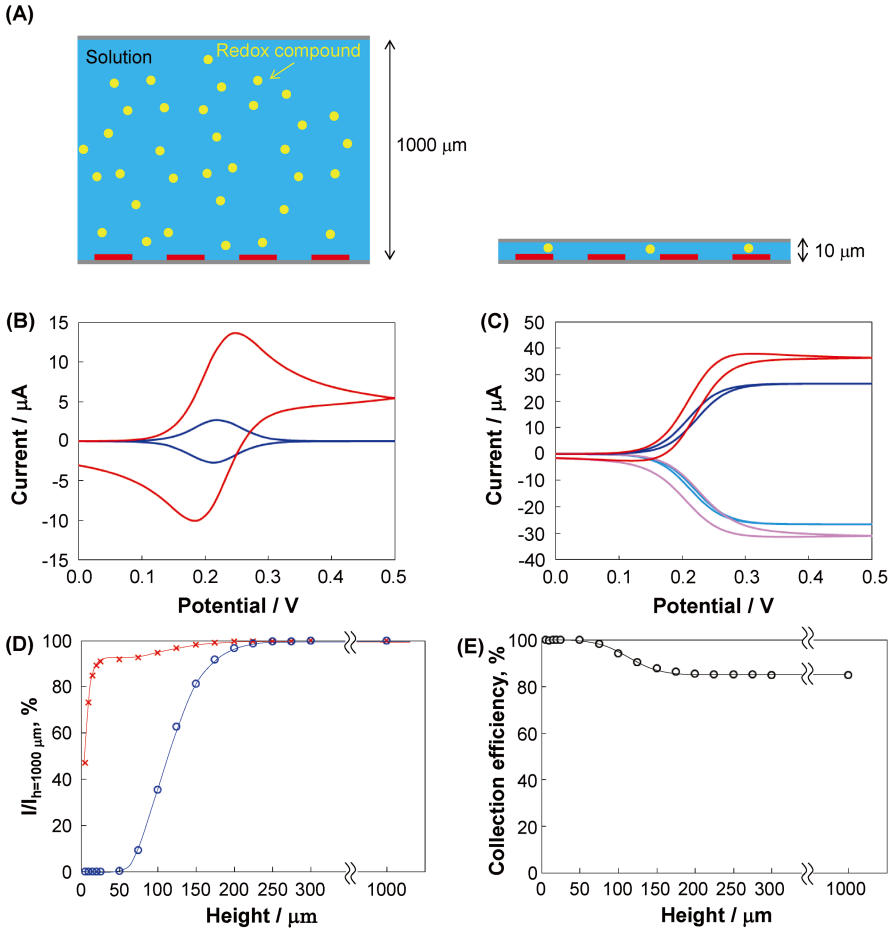

Fig. 5 Results of current simulation based on redox compound diffusion. (A) IDA electrodes were placed on the bottom of models with heights of 1000 and 10 µm. Cyclic voltammograms for 1.0 mM $FcCH_2OH$ in single (B) and dual (C) modes. In single mode, both electrodes were scanned from 0.00 to 0.50 V at 20 mV/s and the response was acquired from one electrode when the channel heights were 1000 (red) and 10 µm (blue). In dual mode, one electrode (generator: 1000 µm, red; 10 µm, blue) was scanned from 0.00 to 0.50 V at 20 mV/s, while the other electrode (collector: 1000 µm, pink; 10 µm, aqua) was held at 0.00 V. (D) Dependence of simulated current on channel height for single (blue) and dual (red) modes. All values are normalized by the value for 1000 µm. (E) Dependence of collection efficiency on channel height.

and 3.30, respectively. From the single-mode cyclic voltammogram, the separation between the oxidation and reduction peaks (ΔE_P) was found to be approximately 60 mV. Figure 3C shows that the electrochemical signals in dual mode were proportional to the concentration of $FcCH_2OH$. Therefore, the device can be used for quantitative detection.

Figures 4(A) and 4(B) show the configuration of the groove in the acrylic resin block and a close-up of the peeled device within the groove, respectively. Single- and dual-mode cyclic voltammograms for $FcCH_2OH$ are shown in Figs. 4(C) and 4(D), respectively. It can be seen that successful redox cycling occurred when the device was inserted into the bent groove in the acrylic resin block. The collection efficiency and the signal amplification ratio were 81.8% and 4.36, respectively. From the single-mode cyclic voltammogram, ΔE_P was found to be about 110 – 180 mV. The current for the bent device was similar to that for the device on the glass slide in dual mode, and it is clear that electrochemical measurements can be successfully performed in narrow spaces using such a flexible device. In contrast, the ΔE_P increased and the currents decreased by bending the device strongly, indicating that the electrodes were cracked. It might be necessary for electrodes to use a metal having high ductility, such as gold.

Compared to other IDA electrodes,[14] the signal amplification and the collection efficiency of the present device are low. For improving the signal amplification and the collection efficiency, it is necessary to modify the geometric features of the electrodes, including their spacing, width, and aspect ratio because the signal amplification and the collection efficiency of IDA electrodes depends on the geometric features.[14]

To analyze the behavior of redox cycling in small spaces precisely, current simulations were performed. Simulations were carried out to determine the effects of confinement on the redox current by varying the channel height in the model, as illustrated schematically in Fig. 5(A). Simulated single- and dual-mode voltammograms are shown in Figs. 5(B) and 5(C), respectively, for channel heights of 1000 and 10 µm. As shown in Fig. 5(B), when the channel height in the model was changed from 1000 to 10 µm, the single-mode current response at 0.50 V decreased from approximately 5.4 to 0 µA because almost all of the redox compound was rapidly consumed during the electrochemical process. In contrast, in dual mode, the current

response at 0.50 V decreased only slightly from approximately 36 to 27 μA, as seen in Fig. 5(C). This is because the redox compound consumed at the generator electrodes was regenerated at the collector electrodes. Thus, IDA electrodes are useful for electrochemical detection in small spaces because of redox compound regeneration.

The dependence of the peak current at 0.50 V on the channel height is shown in Fig. 5(D). In single mode, the current dramatically decreased for channel heights of less than 200 μm, because the $FcCH_2OH/FcCH_2OH^+$ diffusion layer produced by the electrodes extended to the roof of the channel, so that the electrodes received an insufficient supply of $FcCH_2OH$ during the electrochemical reaction. No current was generated in single mode when the channel height was below 50 μm. In contrast, in dual mode, the current decreased by only 8% for a channel height of 50 μm although the diffusion layer produced by the generator electrodes extended to the roof of the channel. A steady-state concentration gradient of $FcCH_2OH/FcCH_2OH^+$ was rapidly formed between the generator and collector electrodes in dual mode, which gave rise to a steady-state current. When the height was 10 – 25 μm, the diffusion layer became thinner and the electrochemical reaction took place mainly at the edges of electrode fingers that were facing each other, leading to a decrease in the current response. Figure 5(E) shows the dependence of the dual-mode collection efficiency at 0.50 V on the channel height. It dramatically increased as the channel height decreased from 1000 to 5 μm, showing that the narrow space is effective at improving the collection efficiency. Thus, the above results indicate that the proposed device is highly promising for electrochemical detection in small spaces.

Comparing Fig. 5(B) and Fig. 3(A), it can be seen that for single mode, the simulated peak current of 14 μA was very similar to the experimentally obtained value of 15 μA. Comparing Fig. 5(C) and Fig. 3(B), the simulated generator current of 36 μA at 0.50 V was very similar to the experimental value of 37 μA in dual mode. Thus, the observed electrochemical behavior was found to be consistent with that predicted by the simulations.

We have previously reported electrochemical imaging devices consisting of IDA electrodes fabricated on glass slides,[9-13] with up to 1024 electrochemical sensors integrated on a single slide.[11] We are now attempting to fabricate similar devices on flexible substrates in order to realize electrochemical imaging of soft materials.

Conclusions

In the present study, an SU-8 layer was used as the substrate for a flexible amperometric device, which incorporated IDA electrodes for electrochemical detection in narrow spaces. During an experimental test in which the device was inserted into a narrow groove, it exhibited a clear electrochemical response based on redox cycling of $FcCH_2OH/FcCH_2OH^+$. Simulations were also carried out, and the results confirmed that effective redox cycling occurred in small spaces. The flexibility of the device makes it highly promising for electrochemical detection in narrow complicated structures.

Acknowledgements

This work was supported in part by a Grant-in-Aid for Scientific Research (A) (No. 25248032) and for Young Scientists (B) (No. 23760745) from the Japan Society for the Promotion of Science (JSPS), and in part by the Cabinet Office, Government of Japan, through its “Funding Program for Next Generation World-Leading Researchers”.

References

1. D. H. Kim, J. Viventi, J. J. Amsden, J. Xiao, L. Vigeland, Y. S. Kim, J. A. Blanco, B. Panilaitis, E. S. Frechette, D. Contreras, D. L. Kaplan, F. G. Omenetto, Y. Huang, K. C. Hwang, M. R. Zakin, B. Litt, and J. A. Rogers, *Nat. Mater.*, **2010**, *9*, 511.
2. J. Viventi, D. H. Kim, L. Vigeland, E. S. Frechette, J. A. Blanco, Y. S. Kim, A. E. Avrin, V. R. Tiruvadi, S. W. Hwang, A. C. Vanleer, D. F. Wulsin, K. Davis, C. E. Gelber, L. Palmer, J. Van der Spiegel, J. Wu, J. Xiao, Y. Huang, D. Contreras, J. A. Rogers, and B. Litt, *Nat. Neurosci.*, **2011**, *14*, 1599.
3. F. J. Rodríguez, D. Ceballos, M. Schüttler, A. Valero, E. Valderrama, T. Stieglitz, and X. Navarro, *J. Neurosci. Methods*, **2000**, *98*, 105.
4. A. Blau, A. Murr, S. Wolff, E. Sernagor, P. Medini, G. Iurilli, C. Ziegler, and F. Benfenati, *Biomaterials*, **2011**, *32*, 1778.
5. H. Kudo, T. Sawada, E. Kazawa, H. Yoshida, Y. Iwasaki, and K. Mitsubayashi, *Biosens. Bioelectron.*, **2006**, *22*, 558.
6. W. Y. Wu, X. Q. Zhong, W. Wang, Q. A. Miao, and J. J. Zhu, *Electrochem. Commun.*, **2010**, *12*, 1600.
7. M. Kaltenbrunner, T. Sekitani, J. Reeder, T. Yokota, K. Kuribara, T. Tokuhara, M. Drack, R. Schwödiauer, I. Graz, S. Bauer-Gogonea, S. Bauer, and T. Someya, *Nature*, **2013**, *499*, 458.
8. O. Niwa, Y. Xu, H. B. Halsall, and W. R. Heineman, *Anal. Chem.*, **1993**, *65*, 1559.
9. K. Ino, T. Nishijo, T. Arai, Y. Kanno, Y. Takahashi, H. Shiku, and T. Matsue, *Angew. Chem., Int. Ed.*, **2012**, *51*, 6648.
10. K. Ino, Y. Kanno, T. Nishijo, T. Goto, T. Arai, Y. Takahashi, H. Shiku, and T. Matsue, *Chem. Commun.*, **2012**, *48*, 8505.
11. K. Ino, W. Saito, M. Koide, T. Umemura, H. Shiku, and T. Matsue, *Lab Chip*, **2011**, *11*, 385.
12. K. Ino, T. Nishijo, Y. Kanno, F. Ozawa, T. Arai, Y. Takahashi, H. Shiku, and T. Matsue, *Electrochemistry*, **2013**, *81*, 682.
13. K. Ino, Y. Kitagawa, T. Watanabe, H. Shiku, M. Koide, T. Itayama, T. Yasukawa, and T. Matsue, *Electrophoresis*, **2009**, *30*, 3406.
14. J. I. Heo, Y. Lim, and H. Shin, *Analyst*, **2013**, *138*, 6404.
15. M. Rahimi and S. R. Mikkelsen, *Anal. Chem.*, **2011**, *83*, 7555.
16. L. Rassaei, P. S. Singh, and S. G. Lemay, *Anal. Chem.*, **2011**, *83*, 3974.
17. K. Toda, S. Hashiguchi, S. Oguni, and I. Sanemasa, *Anal. Sci.*, **1997**, *13*, 981.
18. C. Cannes, F. Kanoufi, and A. J. Bard, *J. Electroanal. Chem.*, **2003**, *547*, 83.
19. B. Jin, W. Qian, Z. Zhang, and H. Shi, *J. Electroanal. Chem.*, **1996**, *411*, 29.
20. S. K. Kim, P. J. Hesketh, C. Li, J. H. Thomas, H. B. Halsall, and W. R. Heineman, *Biosens. Bioelectron.*, **2004**, *20*, 887.